OXFORD

Dissociable neural networks for processing fearful bodily expressions at different spatial frequencies

Maria-Chiara Villa (ID)[1,†], Alessio Borriero (ID)[1,2,3,†], Matteo Diano (ID)[1,4], Tommaso Ciorli (ID)[5], Alessia Celeghin (ID)[1,4],

Beatrice de Gelder (ID)[6,7], and Marco Tamietto (ID)[1,4,8,*]

[1]Department of Psychology, University of Torino, via G. Verdi 10, Torino 10124, Italy
[2]International School of Advanced Studies, University of Camerino, via Gentile III da Varano, Camerino (MC) 62032, Italy
[3]Pegaso Telematic University, Via Porzio, Centro Direzionale, Isola F2, Naples 80143, Italy
[4]Neuroscience Institute of Turin - NIT, via G. Verdi 10, Torino 10124, Italy
[5]SAMBA (SpAtial, Motor and Bodily Awareness) Research Group, Department of Psychology, University of Torino, via G. Verdi 10, Torino 10124, Italy
[6]Department of Cognitive Neuroscience, Faculty of Psychology and Neuroscience, Maastricht University, Oxfordlaan 55, EV 6229, Maastricht, The Netherlands
[7]The Italian Academy for Advanced Studies at Columbia University, 1161 Amsterdam Avenue, New York, NY 10027, United States
[8]Department of Medical and Clinical Psychology, and CoRPS—Center of Research on Psychology in Somatic diseases, Tilburg University, PO Box 90153, Tilburg, LE 5000, The Netherlands

*Corresponding author: Marco Tamietto, Department of Psychology, University of Torino, via G. Verdi 10, Torino 10124, Italy. Email: marco.tamietto@unito.it

[†]Maria-Chiara Villa and Alessio Borriero contributed equally to the work.

The human brain processes visual input across various spatial frequency (SF) ranges to extract emotional cues. Prior studies have extensively explored SF processing in facial expressions, yielding partly conflicting results. However, bodily expressions, which provide complementary emotional and survival-relevant cues, remain unexplored. We investigated the neural mechanisms underlying the processing of low (LSF), high (HSF), and broad spatial frequency (BSF) components in fearful versus neutral bodily postures. Using functional Magnetic Resonance Imaging, we examined brain activity in 20 participants viewing SF-filtered images of bodily expressions in a semi-passive task. A multivariate "searchlight" analysis based on Multi-Voxel Pattern Analysis was employed to decode the non-linear activation patterns associated with each SF band. Our findings reveal that SF processing engages distinct neural networks in response to fearful bodily expressions. BSF stimuli activated a widespread network, including the amygdala, pulvinar, frontal, and temporal cortices. These findings suggest a general threat-detection system integrating information across all SFs. HSF stimuli engaged cortical regions associated with detailed emotional evaluation and motor planning, such as the orbitofrontal cortex, anterior cingulate cortex, and premotor areas, suggesting that processing fine-grained fear cues involves computationally demanding networks related to emotional resonance and action preparation. In contrast, LSF stimuli primarily activated motor-preparatory regions linked to rapid, action-oriented responses, highlighting the brain prioritization of quick readiness to low-detail threats. Notably, the amygdala showed no SF selectivity, supporting its role as a generalized "relevance detector" in emotional processing. The present study demonstrates that the brain flexibly adapts its SF processing strategy based on the visual details available in fearful bodily expressions, underscoring the complexity and adaptability of emotional processing from bodily signals.

Keywords: emotion perception; fearful bodily expressions; spatial frequencies; MVPA; searchlight.

Introduction

The pioneering studies of Joseph LeDoux on threat processing in the rodent auditory system (1998) have fostered countless investigations into the existence of multiple parallel, interacting pathways in the primate visual system that converge on the amygdala (AMG) (e.g. Pessoa and Adolphs 2010; Tamietto and de Gelder 2010). In LeDoux's original formulation, the "low road" is primarily engaged in the coarse and rapid processing of threats, whereas the "high road" is involved in a more refined analysis of stimulus details (LeDoux 1998, 2000). Since the brain processes visual input across a range of spatial frequencies (SFs) to extract critical image statistics (Schyns and Oliva 1999; Chen et al. 2018), filtering emotional images into low (LSF) and high spatial frequency (HSF) components, has become a valuable approach to assess the neural networks preferentially involved in coarse versus detailed visual processing of emotions (Vuilleumier et al.

2003; Winston et al. 2003; Pourtois et al. 2005; Ruiz-Soler and Beltran 2006; Carretié et al. 2007; Delplanque et al. 2007; Rotshtein et al. 2007; Méndez-Bértolo et al. 2016; McFadyen et al. 2017). More specifically, LSF conveys coarse, global information primarily processed by the magnocellular pathway of ancient evolutionary origin. In contrast, HSF carries fine-grained details processed through the parvocellular channels, which emerged more recently in phylogenesis (Livingstone and Hubel 1988; Kauffmann et al. 2014; Cushing et al. 2019; Aghajari et al. 2020).

Prior neuroimaging studies that manipulated SF bands have primarily compared fearful to neutral facial expressions, yielding apparently conflicting results (Vuilleumier et al. 2003; Stein et al. 2014; Skottun 2015; McFadyen et al. 2017; Cushing et al. 2019; Entzmann et al. 2023). Some studies found that AMG responses to fearful expressions, along with superior colliculus and pulvinar activity, were greater for intact or LSF than for HSF faces (Vuilleumier et al. 2003; Canário et al. 2016; Méndez-Bértolo et

2016), thus supporting a subcortical visual pathway in primates that channels coarse fear-related input to the AMG (Tamietto et al. 2012; Méndez-Bértolo et al. 2016; Diano et al. 2017; Celeghin et al. 2019; McFadyen et al. 2019; Méndez et al. 2022). However, other research indicates that AMG responses and those of other emotion-encoding brain regions are nonselective to SFs (McFadyen et al. 2017). These authors propose instead that SF are used flexibly to meet task demands, thus enabling dynamic prioritization based on how "diagnostic" each frequency is for the task at hand (Ruiz-Soler and Beltran 2006; De Gardelle and Kouider 2010). Further hypotheses maintain that clear versus ambiguous threat cues would differentially engage LSF and HSF, respectively (Mermillod et al. 2010; Adams et al. 2011; Cushing et al. 2019), or that SF processing might be lateralized, with the right hemispheres specialized in LSF processing and the left in HSF scene categorization (Kauffmann et al. 2014).

Emotional content is also conveyed by biologically relevant signals other than faces, such as bodily expressions. Just like facial expressions (Bagnis et al. 2019), body language conveys emotions through specific postural configurations, but it also simultaneously suggests the adaptive actions that these emotions typically trigger (de Gelder et al. 2004; de Gelder 2006). Bodily expressions can thus be considered as a bridge between emotion recognition and motor preparation, enabling rapid, context-appropriate behavioral responses (Sinke et al. 2010). For instance, a fearful face signals a threat without indicating a clear coping strategy, whereas a fearful body posture openly indicates whether the subject undertakes a withdrawal, fight or flight response (Kret et al. 2011; Kret et al. 2013; Liang et al. 2019). Moreover, during real-life situations, fearful or angry bodily expressions are better recognized than facial expressions (Abramson et al. 2017) and more readily integrated with contextual social information (e.g. the expressions displayed by the surrounding scene) (Abramson et al. 2021; Kret and de Gelder 2010).

Accordingly, neural processing of bodily expressions aligns with that of facial expressions in some respects but also diverges in critical ways (de Gelder et al. 2011; Kret et al. 2011; Van den Stock et al. 2014; Cao et al. 2018; Cordaro et al. 2020; Lanzilotto et al. 2025). Both involve shared emotional processing networks, such as the amygdala, orbitofrontal cortex (OFC), and anterior cingulate cortex (ACC). However, bodily expressions uniquely engage motor-related areas, including the premotor cortex and supplementary motor area (Hadjikhani and de Gelder 2003; de Gelder et al. 2004; Van den Stock et al. 2011; Pavlova 2012). This integrated network is thought to underlie mechanisms of fear contagion and action preparation in response to observing fear in others (de Gelder et al. 2004; Tamietto and de Gelder 2008; Schiano Lomoriello et al. 2024). These differences in behavioral responses and neural activity suggest that the expectations for SF processing in bodily expressions may differ from those for facial expressions. However, no prior study to date has investigated the potential roles of SF ranges in encoding fear from bodily postures or the neural structures involved.

In the present study, we used functional Magnetic Resonance Imaging (fMRI) to examine the effects of LSF, HFS filtering, and broad-band (broad spatial frequency [BSF]) unfiltered stimuli on the neural encoding of fearful versus neutral bodily expressions. To avoid possible confounds related to different task demands, we employed a semi-passive viewing task in an fMRI block design, where participants simply reported the shift from one image to the next. This design minimizes the attentional and cognitive demands that might have contributed to discrepancies reported in previous studies filtering facial expressions, which involved different paradigms and task demands, including gender or identity evaluations, or required participants to focus attention on specific features like gaze direction (Oliva and Schyns 1997; Schyns and Oliva 1999; Canário et al. 2016).

To isolate brain activations specific to processing fearful versus neutral expressions in relation to different SF bands, we applied the "searchlight" technique, a multivariate machine learning method based on Multi-Voxel Pattern Analysis (MVPA) (Kriegeskorte et al. 2006; Weaverdyck et al. 2020). The searchlight algorithm performs a voxel-wise multivariate classification that accounts for non-linear relationships between voxels (Birn et al. 2001; Deneux and Faugeras 2006), effectively creating local maps of classification accuracy. By scanning the whole brain for voxel clusters with informative patterns, the searchlight approach enables the identification of regions containing information relevant to discriminate among experimental conditions (Haynes 2015), overcoming limitations of traditional mass-univariate statistical approaches like General Linear Models (GLM).

We found that SF processing differentially engages brain networks in response to fearful bodily expressions, with distinct activations for BSF, HSF, and LSF components. Unfiltered BSF stimuli recruited a broad network, including subcortical structures such as the AMG and pulvinar, alongside frontal and temporal cortices, suggesting a general threat-detection role across SF bands. HSF stimuli engaged cortical areas linked to detailed emotional processing, such as the OFC, ACC, and motor-planning regions, suggesting that fear discrimination in HSF stimuli is more computationally demanding, jointly recruiting networks for motor and emotional resonance. In contrast, LSF stimuli primarily activated motor-preparatory regions associated with rapid, action-oriented responses, underscoring the prioritization of quick readiness to low-detail threat cues. The lack of SF selectivity in the AMG, supports its role as a generalized "relevance detector" (Sander et al. 2003; McFadyen et al. 2017).

Materials and methods
Participants
Twenty healthy right-handed participants (16 F; mean age = 21.65 ± 4.15) were recruited. All participants met the MRI inclusion/exclusion criteria and tested negative for any neurologic, psychiatric or psychological condition. Informed consent was obtained from all participants, and the local ethics committee approved the study in accordance with the ethical standards laid down in the Declaration of Helsinki (approval from the University of Torino protocol #121738).

Stimuli
The stimuli consisted of static, grayscale body images of 10 different actors (5 females) depicting either neutral or fearful whole-body expressions, taken from the BEAST dataset (De Gelder and Van Den Stock 2011). Each image measured 500×800 pixels, subtending a visual angle of ~8° × 10.5°, and was transmitted through VisuaStim Digital MR-compatible goggles (EMS Sistemi Elettromedicali, Italy) at a resolution of 800×600 Hz. All original stimuli had a mean luminance of 25 cd/m² (Tamietto et al. 2015), thereby ruling out any influence related to differences in low-level perceptual properties, such as brightness or size. SF filtering was applied to obtain HSF images (high-pass filter cutoff > 24 cycles per image) and LSF images (low-pass filter with a cutoff < 6 cycles per image), while BSF stimuli retained their original frequency content (Vuilleumier et al. 2003) (Fig. 1).
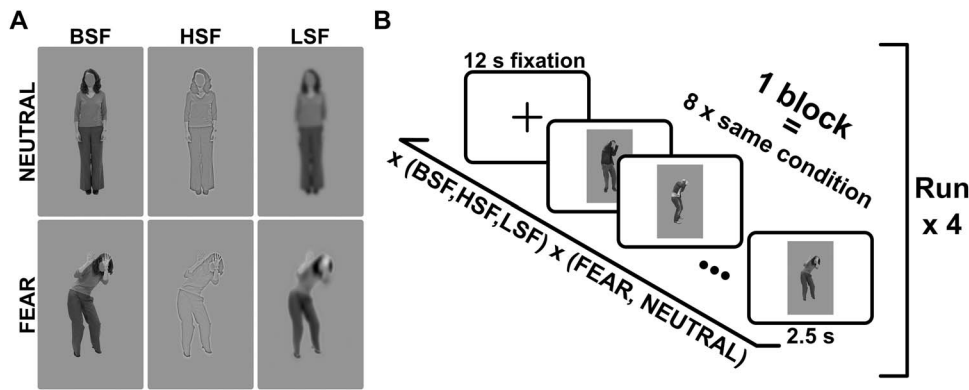
Fig. 1. Examples of fearful and neutral bodily expressions and fMRI paradigm. A) Original images taken from the BEAST dataset displaying intact BSF content were filtered to contain only an HSF or LSF range (de Gelder and Van Den Stock 2011). B) each fMRI session consisted of 4 runs. Each run included 6 blocks of trials, wherein 8 different images expressing the same emotion and spatial frequency were displayed. Each block started with a 12-second fixation cross that served as a rest interval and the body images were presented for 25 seconds.

In addition to physically matching stimulus categories for low-level visual features, we also conducted a separate validation experiment to measure emotion recognition accuracy across SF ranges in participants not enrolled in the fMRI study. Sixty-eight subjects (F = 37, mean age = 28.5 ± 5.9) performed a 3-alternative forced-choice task, identifying emotional expressions (neutral, fearful and happy) regardless of SFs. The emotion discrimination accuracies were: neutral-BSF = 0.93, neutral-LSF = 0.92, neutral-HSF = 0.93; fearful-BSF = 0.97, fearful-LSF = 0.96, fearful-HSF = 0.97. Perceptual sensitivity (d') for the discrimination task was calculated using Signal Detection Theory with the Palamedes Toolbox (Prins and Kingdom 2018), resulting in neutral-BSF mean $d' = 2.07 ± 0.05$ SE, neutral-LSF $d' = 2.05 ± 0.07$ SE, neutral-HSF $d' = 2.08 ± 0.05$ SE; fearful-BSF $d' = 2.20 ± 0.02$ SE, fearful-LSF $d' = 2.14 ± 0.04$ SE, fearful-HSF $d' = 2.18 ± 0.03$ SE. Within each emotion, a repeated measure ANOVA was performed on d' values for each SF, showing that perceptual sensitivity did not significantly differ across the SF ranges (for neutral, $F_{(2,134)} = 0.28$, $P = 0.75$, $\eta_p^2 = 0.004$; for fearful, $F_{(2,134)} = 1.56$, $P = 0.21$, $\eta_p^2 = 0.023$), thus demonstrating that SF manipulation had no significant impact on emotion discrimination and ruling out possible nonspecific effects on fMRI analyses.

Task

The fMRI study was conducted during a single imaging session lasting approximately 52 minutes, divided into four 13-minute runs. Each run consisted of 6 pseudo-randomized blocks, corresponding to one of the following conditions: Neutral-BSF, Fearful-BSF, Neutral-HSF, Fearful-HSF, Neutral-LSF, Fearful-LSF. Each block started with a 12-second fixation cross, followed by 8 different bodily images (each displayed for 2.5 sec), all expressing the same emotion and SF range. To maintain participants' attention, they were required to press a key whenever the image changed within the trial. The experiment was implemented using Presentation® software (Version 18.0, Neurobehavioral Systems, Inc., Berkeley, CA, www.neurobs.com).

Data acquisition and preprocessing

MR images were acquired using a 3 T Ingenia Philips scanner equipped with a 32-channel receiver head-coil. Structural T1-weighted and functional images were obtained with a gradient echo-planar T2 sequence using BOLD (Blood Oxygenation Level Dependency) contrast. A total of 424 functional images (106 time points × 4 runs) were acquired per subject, each consisting of a full brain volume of contiguous axial slices (2.396 × 2.396 × 2.9 mm3). Volumes were collected with a Time Repetition of 2.5 sec and a flip angle of 90°. The preprocessing pipeline was prepared using AFNI (Cox and Hyde 1997) and FSL (FMRIB Software Library) (Jenkinson et al. 2012) commands. Structural images were brain-extracted (*standard_space_roi + bet*), corrected for intensity bias (*3dUnifize*), and spatially normalized to the Montreal Neurological Institute (MNI) space with non-linear registration (*3dQwarp*). Functional volumes underwent slice timing correction (*3dTshift*), realignment to the first volume of each run, and motion correction (*3dvolreg*). Subsequently, all functional volumes were spatially smoothed (*3dBlurToFWHM*) with a 6 mm full-width half-maximum isotropic Gaussian kernel (FWHM) and the signal was normalized (centre: 0; variations in %). Average EPIs were aligned to their high-resolution T1-weighted images and then resampled to the functional acquisition resolution using a weighted sinc-interpolation method.

The fMRI responses of each subject were modeled using the GLM. The GLM design matrix included the onset and duration of each experimental condition, along with six motion parameters obtained from the realignment process to account for the voxel intensity variations due to head movements. Conditions predictors were modeled as blocks lasting 20 sec. and convolved with a double-gamma Hemodynamic Response Function to reflect the brain's BOLD signal.

Searchlight analysis

To isolate brain activity specific to fear processing, we initially subtracted the response evoked by neutral stimuli from fear-related responses within the corresponding SF bands. We then applied the "searchlight" approach to identify brain regions that carry discriminative patterns capable of differentiating fear-specific activity across different SF conditions (Weaverdyck et al. 2020). The most informative voxels were identified using a spherical radius of 10 mm, which is critical for balancing the number of features and avoiding overfitting (Ying 2019). This radius ensured that the number of features (i.e. voxels) was comparable to the number of training samples, thereby optimizing generalization. Subsequently, we built the model to classify activity across the three SF bands: BSF, HSF, and LSF. The dataset for the classification model included four samples per subject per fearful SF condition, resulting in a total of 240 brain volumes.
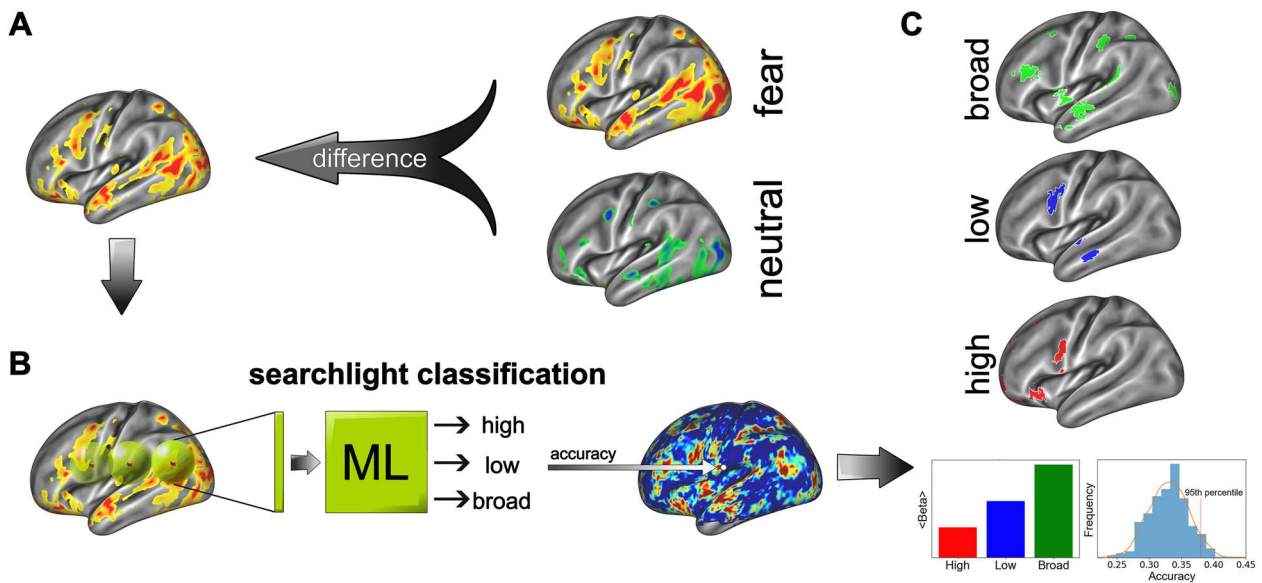
Fig. 2. Searchlight analysis pipeline for fear-related spatial frequency processing. A) the initial step involved isolating brain responses specific to fear processing by subtracting activity evoked by neutral stimuli from fear-related responses within corresponding SF bands. This difference map was used as input for subsequent analyses. B) the searchlight approach was employed to identify brain regions capable of discriminating between the three fearful SF conditions. A support vector machine classified local voxel patterns, generating an accuracy map. Each voxel was assigned an accuracy score, reflecting how well the local voxel patterns can different SF conditions C) to identify significant voxels, a permutation test was conducted and a null accuracy distribution generated for each brain region. Voxels with accuracy >95th percentile of the null distribution were considered significant, and the corresponding brain areas were categorized based on their preferred SF band, as determined by the beta weights of the SF responses.

A Support Vector Machine (SVM) classifier was used to determine whether local voxel patterns could classify the different SF conditions, with voxel features within the searchlight sphere serving as input (Noble 2006; De Martino et al. 2008). Indeed, the SVM aims to find the optimal hyperplane separating the classes corresponding to different SFs. Training and testing of the model employed 4-fold cross-validation (Fushiki 2011). The SVM classification generated accuracy maps (ranging from 0 to 1), reflecting how well different SF conditions could be distinguished based on local voxel patterns.

To identify significant voxels, we applied a more stringent selection criterion than the random-choice accuracy level (0.33 for a three-class problem reflecting three different SFs). An ROI-wise permutation test (Paschali et al. 2022) was performed by shuffling dataset labels and re-running the classification to generate a null accuracy distribution for each brain structure, using the Glasser atlas parcellation (Glasser et al. 2016). Voxels with accuracy above the 95th percentile of the null distribution were considered significant. This yielded an array of region-specific thresholds ranging from $0.334 < P < 0.449$. Finally, after filtering the original searchlight output based on the permutation test, significant voxels were categorized by their preferred SF band (BSF, HSF, LSF) according to which condition produced the highest average activation within each ROI. This approach emphasizes differences in the voxels' responses to the SF bandwidths. Fig. 2 summarizes the entire processing pipeline.

Results

We found that 57% of voxels contained sufficient information to distinguish above chance between the three fear-specific SF activation patterns, with peak accuracy reaching 49,1% in the dorsolateral prefrontal cortex (dlPFC). Fig. 3 illustrates the brain regions identified by the searchlight analysis, with accuracy values for SF differentiation significantly higher than expected

from a null model. Detailed results are reported in Tables 1, 2 and 3.

Fear selectivity for BSF

A distributed network spanning frontal, temporal and occipital regions, along with subcortical structures, significantly differentiated between fearful and neutral bodily expressions in the BSF condition. These regions included core nodes of the emotion-processing network, such as the bilateral AMG, posterior thalamus, rostral and middle cingulate cortex (MCC), anterior insula (INS) and superior temporal gyrus (STG). Additional clusters were observed in the inferior (IFG) and middle frontal (MFG) gyri, overlapping with regions of the dlPFC and the caudal sector of the OFC, bordering the anterior INS.

Other significant regions included primary and associative visual cortices (e.g. fusiform gyrus, STS), parietal areas implicated in attentional orienting and action planning, and pre- and supplementary motor areas. Subcortical structures, including the putamen, pallidum, hippocampus, and cerebellum, were also activated, suggesting their contributions to motor coordination and memory (D'Agata et al. 2011; Van Overwalle et al. 2014; Tamietto et al. 2015).

This activation pattern seemingly implies a broad sensitivity to threat-related signals and aligns with previous fMRI studies using the same stimuli, albeit under different task demands and univariate analyses (Hadjikhani and de Gelder 2003; de Gelder et al. 2004). The engagement of diverse cortical and subcortical regions in BSF processing suggests an integrative, multi-layered approach to assessing threat-related cues.

Fear selectivity for HSF

HSF processing overlapped with BSF in regions like the rostral ACC, anterior INS, and the left fusiform gyrus (FG) but also revealed unique patterns specific to HSF fear encoding. Overall, the HSF condition engaged a more limited set of cortical areas,
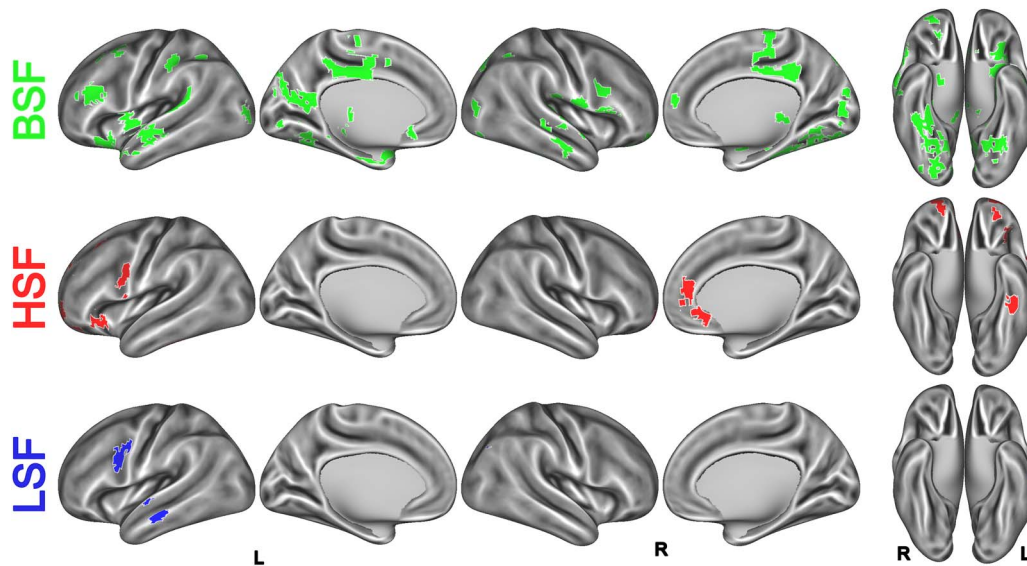
Fig. 3. Significant fear-specific brain regions categorized by spatial frequency preference. Top row: Regions showing significant accuracy for distinguishing fearful from neutral bodily expressions in BSF; middle row: Regions with a significant preference for fear in HSF; bottom row: Regions showing significant accuracy for fear in LSF. The brain maps are presented from lateral, medial, and ventral views, with left (L) and right (R) hemispheres labeled accordingly.

primarily within the frontal lobe, while parietal, occipital and subcortical structures, including the AMG, were not significantly activated. Discriminative regions in HSF included ventral premotor and motor areas, such as the inferior frontal junction (IFJ) and the opercular part of the IFG. Medially, HSF processing extended more dorsally in the rostral ACC, reaching into the vmPFC compared to BSF sites.

Fear selectivity for LSF

LSF-related fear processing revealed frontal activity restricted to ventral premotor and motor cortices, with locations similar to those active during HSF discrimination. Additional significant responses were found in the superior part of the middle temporal gyrus (MTG), bordering the inferior banks of the STS, and in the posterior angular gyrus, adjacent to the inferior intraparietal sulcus (IPS).

Functional comparison across SF bands

To facilitate functional comparison across SF bands and examine how each SF selectively engages brain networks when processing fearful stimuli, we grouped activated areas according to their predominant roles, following the previous classification by de Gelder et al. (2004). Regions activated within each SF band were categorized into visual processing, emotional processing, action representation and motor response clusters, then normalized by the total number of regions identified in each SF band (Fig. 4).

This comparative analysis reveals distinct processing networks for each SF band. BSF stimuli activate a broad, integrative network with a balanced combination of visual processing, emotional evaluation, and motor and premotor-related functions, thus highlighting a comprehensive response. In contrast, HSF stimuli recruit a more selective network centered on cortical areas for detailed emotional evaluation and motor planning, reflecting increased needs for fine-grained threat processing. Finally, LSF stimuli prioritize action-oriented responses, emphasizing regions associated with quick motor preparation and coarse visual analysis.
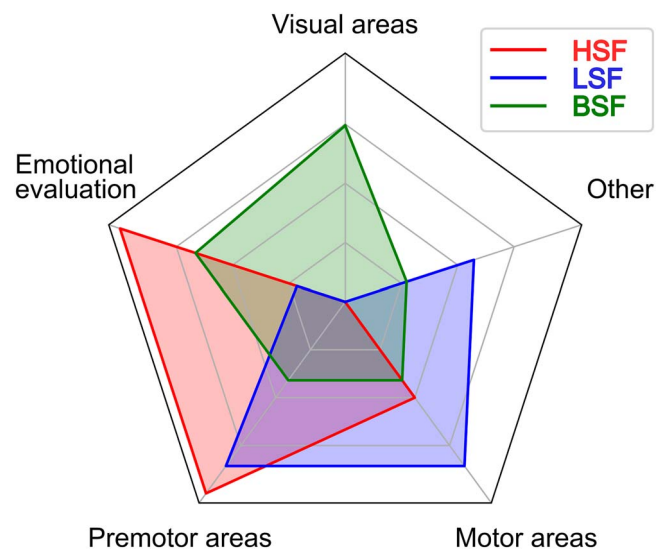

Fig. 4. Functional differentiation of brain networks by SF bands during fear processing. The radar plot illustrates the distribution of brain regions activated by each SF band in terms of their predominant functional roles according to de Gelder et al. (2004).

Discussion

In the present study, we investigated for the first time how SF processing influences the perception of fearful bodily stimuli, revealing the differential engagement of brain networks across BSF, HSF, and LSF bands. Using MVPA, we decoded non-linear activation patterns and identified neural maps specific to each SF band in relation to fear processing. Our sample size is consistent with prior neuroimaging studies using searchlight MVPA (Kriegeskorte et al. 2006; Chen et al. 2011; Soon et al. 2013) or analyzing SF sensitivity to facial expressions with general linear models (Goffaux et al. 2011; McFadyen et al. 2019; Rotshtein et al. 2007; Vuilleumier et al. 2003; Winston et al. 2003; Yue et al. 2006; Zhao et al. 2023). Nevertheless, larger samples could provide

Table 1. Significant fear-specific clusters in BSF. The nomenclature of brain areas was derived by overlapping the maps with the CA_ML_18 atlas (Eickhoff Zilles macro labels from the MNI N27 Atlas) (Eickhoff et al. 2005), available in AFNI libraries. The coordinates follow the LPI orientation.

BSF								
Lobe	Surface	N. Voxels	MNI Coordinates			Intersection with atlas CA_M18	Hemisphere	Brain area
			X	Y	Z			
Temporal								
	Mesial	152	−47.7	−11.7	0	61.80%	L	STG
		54	32.5	−34.2	−17.8	89%		MTG
		46	−39.8	0.3	12.5	46.50%		INS
		55	47.8	−25.7	14.9	52%	R	STG
	Lateral	266	−36.1	18.3	−19.2	35.30%	L	Temporal pole
		60	−61.8	−43.4	19.1	66.50%		STG
		21	−54.7	6.2	−24.9	86.70%		MTG
		44	62.4	−6.6	−19.3	92.80%	R	MTG
		25	62.9	−16.1	−7.3	75.10%		STG
Occipital								
	Mesial	168	−24.7	−59.2	13.2	42.90%	L	Fusiform gyrus
						31%		Lingual gyrus
		106	−9.9	−59.6	14.2	51.10%		Calcarine gyrus
						34.80%		Precuneus
		36	−0.1	−84	−0.4	70.40%		Calcarine gyrus
		186	26.8	−50.4	−15.1	56.40%	R	Fusiform gyrus
		43	20.4	−76.3	−12.2	55.70%		Lingual gyrus
		25	22.8	−86.8	−12.9	81%		Lingual gyrus
		25	11.2	−81.3	10.3	95.50%		Calcarine gyrus
		22	26.7	−70.8	41.7	81.40%		Superior Occipital gyrus
		17	4.4	−83.3	23.8	65.70%		Cuneus
	Lateral	92	−16	−77.8	28.4	53%	L	Superior Occipital gyrus
						31.60%		Cuneus
		39	−37.8	−87.3	7.7	94.10%		MTG
		54	−55.7	−12.3	−9.8	85.70%	R	Fusiform gyrus
		16	39.5	−80.7	−14.4	74.40%		Inferior Occipital gyrus
		16	34	−60.2	−21	70.70%		Cerebellum(VI)
						30.00%		Fusiform gyrus
		15	22.7	−100.8	10.8	52.30%		Superior Occipital gyrus
Frontal								
	Mesial	225	−1.4	−25.2	40.1	70.40%	L	MCC
		23	−5.2	27.3	−13.4	38.50%		Rectal gyrus
						33.40%		Middle Orbital gyrus
		20	−27.7	22.5	50.2	100%		Middle Frontal gyrus
		46	−39.8	0.3	12.5	53.60%	R	Rolandic Operculum
		45	2.2	−23.3	65.8	42.20%		Paracentral Gyrus
		32	3.9	52.8	14.9	35.90%		Superior Medial
						30.10%		ACC
	Lateral	30	10.8	−20.8	47.3	73.90%		MCC
		266	−36.1	18.3	−19.2	30%	L	IFG (p.orbitalis)
		92	−35.2	10.9	57.5	78.70%		MFG
		91	−45.1	31.8	22.6	77%		IFG (p.Triangularis)
						15.40%		MFG
		57	57.9	3.3	3.2	45.40%		Rolandic Operculum
		26	−50.9	19.7	27.1	100%		IFG (p.Triangularis)
		23	60.4	−7.4	9	63.70%	R	IFG (p.Opercularis)
		22	52.8	17.3	1.3	53.10%		Rolandic Operculum
						30.80%		IFG (p.Triangularis)
		18	59	19.4	9.3	71.60%		IFG (p.Opercularis)
		15	44.9	10.7	26.1	86.70%		IFG (p.Opercularis)
	Orbital	32	29	54.3	−15.7	88.10%	R	Middle Orbital gyrus
		23	24.7	36.3	−19.8	57.10%		Middle Orbital gyrus
Parietal								
	Mesial	16	31.7	−53.3	41.6	65.10%	R	Angular gyrus
	Lateral	16	−46.7	−29.4	38.8	76.80%	L	Inferior Parietal Lobule

(Continued)

Table 1. Continued

BSF								
Lobe	**Surface**	**N. Voxels**	**MNI Coordinates**			**Intersection with atlas CA_M18**	**Hemisphere**	**Brain area**
			X	**Y**	**Z**			
Subcortical								
		75	−23.4	−5.4	−21	39.50%	L	AMG
						31.70%		Hippocampus
		72	−16.8	−27.9	5.8	72.20%		Thalamus
		24	−29.7	−3.1	3.5	86.30%		Putamen
		21	−17.5	2.5	−1.3	98.10%		Pallidum
		90	1.21	−4.9	2.8	68.20%	R	Putamen
		40	18.9	−22.3	4	100%		Thalamus
		31	11.9	−28.9	7.7	78.70%		Thalamus
		31	14.8	−73.5	52.4	69.10%		SPL
						30.90%		Precuneus
		16	24.4	−7.7	−12.4	42.60%		AMG
						39.20%		Hippocampus

Table 2. Significant fear-specific clusters in HSF.

HSF								
Lobe	**Surface**	**N. Voxels**	**MNI Coordinates**			**Intersection with atlas CA_M18**	**Hemisphere**	**Brain area**
			X	**Y**	**Z**			
Temporal								
	Mesial	34	−43	−28.9	−22.9	95.40%	L	ITG
Frontal								
	Mesial	43	−35.3	25.2	−5.5	51.40%	L	IFG (p.orbitalis)
						41.90%		INS
		38	−27.9	58	−2.9	58%		Superior Orbital gyrus
		33	−25.6	44	38.8	65.50%		Superior Frontal gyrus
		28	−28	43.2	−15.1	68.80%		Middle Orbital gyrus
		39	4.1	33.2	−9.2	53.50%	R	Middle Orbital gyrus
		38	9	43	12.3	94.10%		ACC
		31	18.5	54	−18.9	65.30%		Middle Orbital gyrus
		22	24.5	60.9	−9.9	59.90%		Superior Orbital gyrus
		15	3.5	17.1	51.1	51.30%		SMA
	Lateral							
		40	−51.4	8	26.3	72.70%	L	Precentral gyrus
		20	−42.5	42.3	3.4	54.60%		IFG (p.triangularis)
		19	−25.2	23	45.5	96.60%		Middle Frontal gyrus
		15	−59.1	9.4	6.8	56.10%		IFG (p.Opercularis)

Table 3. Significant fear-specific clusters in LSF.

LSF								
Lobe	**Surface**	**N. Voxels**	**MNI Coordinates**			**Intersection with atlas CA_M18**	**Hemisphere**	**Brain area**
			X	**Y**	**Z**			
Temporal								
	Lateral	68	−64.2	−14.9	−11.6	93.50%	L	MTG
Occipital								
	Lateral	15	43	−75.4	42.7	78.70%	R	Angular gyrus
Frontal								
	Lateral	29	−43.8	3	29.2	59.90%	L	Precentral gyrus
						40.10%		IFG (p.Opercularis)

additional insights into individual differences in SF sensitivity (Dubois and Adolphs 2016), such as variations related to gender, psychological traits and dispositions, or hemispheric laterality (Phillips et al. 2003; Wager et al. 2003; Palomero-Gallagher and Amunts 2022). Nonetheless, the positive results reported here are supported by metrics that inherently account for the sample size, ensuring the generalizability and validity of findings (Geirhos et al. 2018; Geirhos et al. 2020). Therefore, our findings extend previous observations on facial expressions and highlight the unique role of bodily expressions in threat detection, as they convey emotional cues closely tied to response programs essential for survival (de Gelder et al. 2004).

Observing fearful body stimuli in the BSF condition activated a broad integrative network spanning frontal, temporal, and visual regions, as well as subcortical structures. Key areas included the bilateral AMG, posterior thalamus (in a location compatible with the pulvinar), cingulate cortex, INS, and STG. However, while we observed this widespread network for BSF fearful bodies, we did not find the selective amygdala engagement for LSF stimuli that might have been anticipated based on prior work with faces (Vuilleumier et al. 2003; Méndez-Bértolo et al. 2016). This activation pattern suggests a generalized contribution of the AMG to threat detection that incorporates both LSF and HSF information. It also suggests that amygdala findings on SF tuning derived from facial expression studies may not straightforwardly generalize to body postures, particularly considering intracranial evidence that the amygdala can respond differently even to specific face parts (Meletti et al. 2012). The absence of specific AMG selectivity for either HSF or LSF stimuli indicates that its activity facilitates the detection of potential threats across a range of visual details rather than being specific for coarse signals, at least in relation to bodily signals (Sander et al. 2003; McFadyen et al. 2017). Furthermore, the "diagnostic approach" suggests that the brain flexibly prioritizes SF processing based on task demands, with HSF demanding more detailed processing and LSF facilitating rapid action (Ruiz-Soler and Beltran 2006; De Gardelle and Kouider 2010). This flexibility aligns with the AMG role as a "relevance detector" that quickly assesses emotionally salient information across all SFs (Sander et al. 2003; Phelps and LeDoux 2005).

The distributed activation is in keeping with prior research on emotional body perception, suggesting that perceiving BSF fearful bodies triggers adaptive, evolutionarily rooted responses that bridge emotion with motor action, enabling timely behavioral responses (Hadjikhani and de Gelder 2003; de Gelder et al. 2004; Van Den Stock et al. 2011). This tenet is further supported by discriminative activity in motor-related areas, including the supplementary motor area (SMA), premotor cortex and basal ganglia, which mediate action-preparedness for context-appropriate responses to fearful stimuli (Van Overwalle et al. 2014; Borgomaneri et al. 2015a). In fact, motor and emotional resonance are both integral to processing social and emotional cues, with motor areas supporting action readiness, while regions like AI and ACC contribute to interoceptive awareness and motor resonance (Tamietto et al. 2015; Del Vecchio et al. 2024).

During fear discrimination in HSF stimuli, we observed distinct activations in cortical regions involved in high-level emotional processing and evaluation, including the OFC, ACC, anterior INS, and IFG. The ACC role in conflict regulation and fear conditioning is coherent with its heightened activation for HSF stimuli, which demand detailed emotional evaluation (Holroyd and Verguts 2021). Accordingly, lesions in the ACC lead to impairments in processing nuanced emotional information (Hornak 2003). This cortical preference for fine-grained processing is

consistent with studies on facial expressions reporting that HSF stimuli are computationally demanding and engage additional cortical areas related to emotional evaluation and executive control (Ruiz-Soler and Beltran 2006; De Gardelle and Kouider 2010). Notably, the OFC selective activation for HSF stimuli suggests its contribution to higher-level functions in emotional decision-making and the integration of reward-based information (Sander et al. 2003; Ferrari et al. 2015).

The HSF condition also activated motor planning regions, including the ventral premotor IFJ and the opercular IFG, highlighting an overlap with action-related processing regions. The IFJ is involved in non-spatial attention and biases perception through neural synchrony with associative visual areas (Asplund et al. 2010; Baldauf and Desimone 2014). Moreover, passive observation of fearful facial expressions modulates intracranially recorded activity in prefrontal/insular regions and motor territories, coherent with the present results (Del Vecchio et al. 2024). Subsequent electrical stimulation in the former sites evoked emotional and interoceptive responses, whereas opercular stimulation evoked sensorimotor responses (Del Vecchio et al. 2024). These results suggest that fear discrimination based on impoverished HSF stimuli relies on motor engagement for action recognition and emotional resonance through parallel but interacting networks (Niedenthal et al. 2010; Palagi et al. 2020; Caruana 2022; Sessa et al. 2022; Schiano et al. 2023).

In the LSF condition, fearful stimuli primarily recruited motor-preparatory regions similar to those activated in HSF discrimination. In contrast, ACC and insular regions were not recruited, thus suggesting a reliance on motor resonance that likely reflects the brain prioritization of rapid motor planning in response to low-detail threat cues. Activations also included MTG/STS and the angular gyrus/IPS, reflecting biological motion processing and body perception. The STS has been proposed as the terminal site of a third visual pathway specialized for the dynamic aspects of social perception (Pavlova 2012; Pitcher and Ungerleider 2021). The angular gyrus/IPS has been implicated as an integrative hub for attentional shift and stimulus representation from feature selection (Xu and Chun 2009). These findings indicate that early motor resonance can serve as a swift defensive mechanism when the visual input is coarse or ambiguous, supporting rapid action decisions before full emotional appraisal unfolds. This underscores a key advantage of LSF-based processing: the facilitation of immediate behavioral strategies for threat avoidance or confrontation, illustrating how motor resonance bridges perception and action under time-critical conditions (Rizzolatti and Sinigaglia 2016).

A substantial body of literature highlights the role of hemispheric lateralization in SF processing (Proverbio et al. 1997; Peyrin et al. 2003; Howard and Reggia 2007; Awasthi et al. 2011). Specifically, prior studies suggest that LSFs are predominantly processed in the right hemisphere, whereas HSFs are processed in the left hemisphere (Kauffmann et al. 2014). However, it remains unclear whether these lateralization principles apply consistently across stimulus categories and contexts. Our findings challenge the generality of this model by revealing a left-hemisphere preference for LSFs primarily associated with motor and premotor clusters. One plausible explanation is that, since all our participants were right-handed, the dominant hemisphere might preferentially process defensive motor responses prompted by seeing fearful bodily actions. This interpretation is supported by initial evidence measuring cortico-spinal excitability in response to such stimuli (Borgomaneri et al. 2015b).

Our results reveal that, when processing fearful bodily expressions, the brain engages structures associated with high-level emotional coding in response to HSFs, while LSF stimuli predominantly activate motor-related areas. Interestingly, motor planning regions are also activated in response to HSF stimuli. This finding contrasts with prior observations in facial processing and underscores the importance of movement strategies in responding to fearful emotional contexts. To this end, our study adds nuance to the existing literature. Although face-based models often highlight a clear dissociation between coarse (LSF) and detailed (HSF) pathways, bodily signals appear to engage motor resonance across both SF bands, suggesting a more flexible, context-driven interplay between emotional evaluation and action readiness.

In real-world scenarios, faces are typically viewed at close range during one-to-one interactions, activating neural mechanisms dedicated to understanding and inferring others' mental states (Megías et al. 2020). In contrast, interactions involving bodies can be more indirect, reflecting a distinct dynamic in how bodily information is processed and interpreted. When encountering an emotional bodily expression, a strategy focused on reacting to, or interacting with, the environment appears more critical than inferring the emotional state. This prioritization becomes particularly evident under suboptimal viewing conditions, such as when relying on LSFs, which are crucial for quickly assessing the potentially dangerous valence of the stimuli. From an ecological perspective, this suggests that motor resonance may be evolutionarily tuned to detect and respond to distant or ambiguous threats, highlighting the brain's capacity to optimize survival-related behavior in rapidly changing or uncertain environments (Mobbs et al. 2007). However, when detailed visual information is available through HSFs, the brain activates high-level areas involved in advanced emotional processing alongside motor planning regions. This illustrates the integration of emotional understanding and preparatory action (Del Vecchio et al. 2024), enriching our understanding of the interplay between sensory, motor, and emotional processing in response to fearful stimuli. Moreover, convergent evidence suggests that mirror mechanisms differ for face- vs. limb-related actions (Ferrari et al. 2017), indicating that the neural pathways for bodily postures may be partially distinct. This highlights the need to further investigate connectivity between temporo-occipital and frontal areas to clarify the route by which emotional body cues recruit motor and higher-order cortical networks.

Overall, these findings illustrate a potential mechanistic basis for motor resonance, wherein subcortical threat detection may rapidly engage sensorimotor circuits that interface with cortical emotional networks when processing fearful bodily signals (Tamietto et al. 2009; Rizzolatti and Sinigaglia 2016). By linking bodily cues to both reflexive motor responses and nuanced emotional interpretation, motor resonance emerges as a critical bridge connecting early threat perception with appropriate survival-oriented actions. The present results also expand current knowledge on SF processing by suggesting that its evolutionary role in facilitating rapid threat responses is intricately tied to the ecological context of perceived stimuli. The brain utilization of SF information is shaped by the immediacy and nature of the environmental stimuli, highlighting an adaptive mechanism that prioritizes efficient sensory-motor integration and emotional evaluation based on situational demands, in line with the "diagnostic approach" (Ruiz-Soler and Beltran 2006; De Gardelle and Kouider 2010).

We did not find a clear dorsal-ventral distinction for LSF and HSF stimuli, contrasting the traditional notion that the magnocellular (M) and parvocellular (P) pathways map directly onto the dorsal and ventral streams, respectively (Goodale and Milner 1992; Merigan and Maunsell 1993). The M and P pathways remain highly segregated in subcortical structures, such as the lateral geniculate nucleus. However, as they ascend into cortical regions, the distinction becomes progressively less clear, with inputs from both pathways converging as early as in V1, and further merging in V2 and V3 (Lyon and Kaas 2001; Callaway 2005). Mounting evidence suggests that both M and P inputs contribute to ventral and dorsal streams when visual information reaches higher-level areas (Bullier 2001; Milner and Goodale 2008; Nassi and Callaway 2009). This cortical integration likely supports our finding that LSF and HSF conditions engage partly overlapping networks without strict dorsal-ventral separation. This suggests a more integrated processing mode across SF bands in the cortex.

In conclusion, our findings show that the brain flexibly adapts its SF processing strategy according to the nature of the emotional stimulus, including the SF components available for detecting fearful bodily expressions. This study extends the current understanding of fear processing in different SF bands beyond facial expressions, providing initial insights into how the brain interprets complex bodily cues to detect threats across varying levels of visual details.

Author contributions

Maria Chiara Villa (Formal analysis, Investigation, Validation, Writing—original draft), Alessio Borriero (Data curation, Formal analysis, Methodology, Software, Writing—original draft), Matteo Diano (Data curation, Formal analysis, Funding acquisition, Investigation, Methodology, Resources, Software, Supervision, Validation), Tommaso Ciorli (Methodology, Resources, Software, Validation), Alessia Celeghin (Data curation, Formal analysis, Investigation, Methodology, Supervision), Beatrice de Gelder (Conceptualization, Data curation, Resources, Validation, Writing—review & editing), Marco Tamietto (Conceptualization, Funding acquisition, Investigation, Methodology, Resources, Supervision, Writing—original draft, Writing—review & editing).

Funding

Disclosure

MT has served as Associate Editor for Cerebral Cortex since 1 January 2025 and has recused himself from all editorial decisions related to this manuscript. Full peer review was overseen by Reviewing Editor Daniela Schiller.

References

Abramson L, Marom I, Petranker R, Aviezer H. 2017. Is fear in your head? A comparison of instructed and real-life expressions of emotion in the face and body. *Emotion*. 17:557–565. https://doi.org/10.1037/emo0000252.

Abramson L, Petranker R, Marom I, Aviezer H. 2021. Social interaction context shapes emotion recognition through body language, not facial expressions. *Emotion*. 21:557–568. https://doi.org/10.1037/emo0000718.

Adams RB et al. 2011. Differentially tuned responses to restricted versus prolonged awareness of threat: a preliminary fMRI investigation. *Brain Cogn*. 77:113–119. https://doi.org/10.1016/j.bandc.2011.05.001.

Aghajari S, Vinke LN, Ling S. 2020. Population spatial frequency tuning in human early visual cortex. *J Neurophysiol*. 123:773–785. https://doi.org/10.1152/jn.00291.2019.

Asplund CL, Todd JJ, Snyder AP, Marois R. 2010. A central role for the lateral prefrontal cortex in goal-directed and stimulus-driven attention. *Nat Neurosci*. 13:507–512. https://doi.org/10.1038/nn.2509.

Awasthi B, Friedman J, Williams MA. 2011. Faster, stronger, lateralized: low spatial frequency information supports face processing. *Neuropsychologia*. 49:3583–3590. https://doi.org/10.1016/j.neuropsychologia.2011.08.027.

Bagnis A, Celeghin A, Mosso CO, Tamietto M. 2019. Toward an integrative science of social vision in intergroup bias. *Neurosci Biobehav Rev*. 102:318–326. https://doi.org/10.1016/j.neubiorev.2019.04.020.

Baldauf D, Desimone R. 2014. Neural mechanisms of object-based attention. *Science*. 344:424–427. https://doi.org/10.1126/science.1247003.

Birn RM, Saad ZS, Bandettini PA. 2001. Spatial heterogeneity of the nonlinear dynamics in the FMRI BOLD response. *NeuroImage*. 14:817–826. https://doi.org/10.1006/nimg.2001.0873.

Borgomaneri S, Vitale F, Gazzola V, Avenanti A. 2015a. Seeing fearful body language rapidly freezes the observer's motor cortex. *Cortex*. 65:232–245. https://doi.org/10.1016/j.cortex.2015.01.014.

Borgomaneri S, Vitale F, Avenanti A. 2015b. Early changes in corticospinal excitability when seeing fearful body expressions. *Sci Rep*. 5:14122.

Bullier J. 2001. Integrated model of visual processing. *Brain Res Rev*. 36:96–107. https://doi.org/10.1016/S0165-0173(01)00085-6.

Callaway EM. 2005. Structure and function of parallel pathways in the primate early visual system. *J Physiol*. 566:13–19. https://doi.org/10.1113/jphysiol.2005.088047.

Canário N, Jorge L, Loureiro Silva MF, Alberto Soares M, Castelo-Branco M. 2016. Distinct preference for spatial frequency content in ventral stream regions underlying the recognition of scenes, faces, bodies and other objects. *Neuropsychologia*. 87:110–119. https://doi.org/10.1016/j.neuropsychologia.2016.05.010.

Cao L, Xu J, Yang X, Li X, Liu B. 2018. Abstract representations of emotions perceived from the face, body, and whole-person expressions in the left postcentral gyrus. *Front Hum Neurosci*. 12:419. https://doi.org/10.3389/fnhum.2018.00419.

Carretié L, Hinojosa JA, López-Martín S, Tapia M. 2007. An electrophysiological study on the interaction between emotional content and spatial frequency of visual stimuli. *Neuropsychologia*. 45:1187–1195. https://doi.org/10.1016/j.neuropsychologia.2006.10.013.

Caruana F. 2022. Two simulation systems in the human frontal cortex? Disentangling between motor simulation and emotional mirroring using laughter. *Cortex*. 148:215–217. https://doi.org/10.1016/j.cortex.2021.09.011.

Celeghin A, Galetto V, Tamietto M, Zettin M. 2019. Emotion recognition in low-spatial frequencies is partly preserved following traumatic brain injury. *Biomed Res Int*. 2019:1–10. https://doi.org/10.1155/2019/9562935.

Chen Y et al. 2011. Cortical surface-based searchlight decoding. *NeuroImage*. 56:582–592. https://doi.org/10.1016/j.neuroimage.2010.07.035.

Chen C-Y, Sonnenberg L, Weller S, Witschel T, Hafed ZM. 2018. Spatial frequency sensitivity in macaque midbrain. *Nat Commun*. 9:2852. https://doi.org/10.1038/s41467-018-05302-5.

Cordaro DT et al. 2020. The recognition of 18 facial-bodily expressions across nine cultures. *Emotion*. 20:1292–1300. https://doi.org/10.1037/emo0000576.

Cox RW, Hyde JS. 1997. Software tools for analysis and visualization of fMRI data. *NMR Biomed*. 10:171–178. https://doi.org/10.1002/(SICI)1099-1492(199706/08)10:4/5<171::AID-NBM453>3.0.CO;2-L.

Cushing CA, Im HY, Adams RB Jr, Ward N, Kveraga K. 2019. Magnocellular and parvocellular pathway contributions to facial threat cue processing. *Soc Cogn Affect Neurosci*. 14:151–162. https://doi.org/10.1093/scan/nsz003.

D'Agata F et al. 2011. The recognition of facial emotions in spinocerebellar ataxia patients. *Cerebellum*. 10:600–610. https://doi.org/10.1007/s12311-011-0276-z.

De Gardelle V, Kouider S. 2010. How spatial frequencies and visual awareness interact during face processing. *Psychol Sci*. 21:58–66. https://doi.org/10.1177/0956797609354064.

de Gelder B. 2006. Towards the neurobiology of emotional body language. *Nat Rev Neurosci*. 7:242–249. https://doi.org/10.1038/nrn1872.

de Gelder B et al. 2011. Faces, bodies, social vision as agent vision, and social consciousness. *The science of social vision, Oxford series in visual cognition*. p. 51–74. https://doi.org/10.1093/acprof:oso/9780195333176.003.0004.

de Gelder B, Van Den Stock J. 2011. The bodily expressive action stimulus test (BEAST). Construction and validation of a stimulus basis for measuring perception of whole body expression of emotions. *Front Psychol*. 2:181. https://doi.org/10.3389/fpsyg.2011.00181.

de Gelder B, Snyder J, Greve D, Gerard G, Hadjikhani N. 2004. Fear fosters flight: a mechanism for fear contagion when perceiving emotion expressed by a whole body. *Proc Natl Acad Sci*. 101:16701–16706. https://doi.org/10.1073/pnas.0407042101.

De Martino F et al. 2008. Combining multivariate voxel selection and support vector machines for mapping and classification of fMRI spatial patterns. *NeuroImage*. 43:44–58. https://doi.org/10.1016/j.neuroimage.2008.06.037.

Del Vecchio M et al. 2024. Anatomo-functional basis of emotional and motor resonance elicited by facial expressions. *Brain*. 147:3018–3031. https://doi.org/10.1093/brain/awae050.

Delplanque S, N'diaye K, Scherer K, Grandjean D. 2007. Spatial frequencies or emotional effects? *J Neurosci Methods*. 165:144–150. https://doi.org/10.1016/j.jneumeth.2007.05.030.

Deneux T, Faugeras O. 2006. Using nonlinear models in fMRI data analysis: model selection and activation detection. *NeuroImage*. 32:1669–1689. https://doi.org/10.1016/j.neuroimage.2006.03.006.

Diano M et al. 2017. Dynamic changes in amygdala psychophysiological connectivity reveal distinct neural networks for facial expressions of basic emotions. *Sci Rep*. 7:45260. https://doi.org/10.1038/srep45260.

Dubois J, Adolphs R. 2016. Building a science of individual differences from fMRI. *Trends Cogn Sci*. 20:425–443. https://doi.org/10.1016/j.tics.2016.03.014.

Eickhoff SB et al. 2005. A new SPM toolbox for combining probabilistic cytoarchitectonic maps and functional imaging data. *NeuroImage*. 25:1325–1335. https://doi.org/10.1016/j.neuroimage.2004.12.034.

Entzmann L, Guyader N, Kauffmann L, Peyrin C, Mermillod M. 2023. Detection of emotional faces: the role of spatial frequencies and local features. *Vis Res*. 211:108281. https://doi.org/10.1016/j.visres.2023.108281.

Ferrari C, Lega C, Tamietto M, Nadal M, Cattaneo Z. 2015. I find you more attractive … after (prefrontal cortex) stimulation. *Neuropsychologia*. 72:87–93. https://doi.org/10.1016/j.neuropsychologia.2015.04.024.

Ferrari PF, Gerbella M, Coudé G, Rozzi S. 2017. Two different mirror neuron networks: the sensorimotor (hand) and limbic (face) pathways. *Neuroscience*. 358:300–315. https://doi.org/10.1016/j.neuroscience.2017.06.052.

Fushiki T. 2011. Estimation of prediction error by using K-fold cross-validation. *Stat Comput*. 21:137–146. https://doi.org/10.1007/s11222-009-9153-8.

Geirhos R et al. 2018. Generalisation in humans and deep neural networks. *Neural Information Processing Systems*. 31:7549–7756. https://doi.org/10.15496/publikation-30814.

Geirhos R et al. 2020. Shortcut learning in deep neural networks. *Nat Mach Intell*. 2:665–673. https://doi.org/10.1038/s42256-020-00257-z.

Glasser MF et al. 2016. A multi-modal parcellation of human cerebral cortex. *Nature*. 536:171–178. https://doi.org/10.1038/nature18933.

Goffaux V et al. 2011. From coarse to fine? Spatial and temporal dynamics of cortical face processing. *Cereb Cortex*. 21:467–476. https://doi.org/10.1093/cercor/bhq112.

Goodale MA, Milner AD. 1992. Separate visual pathways for perception and action. *Trends Neurosci*. 15:20–25. https://doi.org/10.1016/0166-2236(92)90344-8.

Hadjikhani N, de Gelder B. 2003. Seeing fearful body expressions activates the fusiform cortex and amygdala. *Curr Biol*. 13:2201–2205. https://doi.org/10.1016/j.cub.2003.11.049.

Haynes J-D. 2015. A primer on pattern-based approaches to fMRI: principles, pitfalls, and perspectives. *Neuron*. 87:257–270. https://doi.org/10.1016/j.neuron.2015.05.025.

Holroyd CB, Verguts T. 2021. The best laid plans: computational principles of anterior cingulate cortex. *Trends Cogn Sci*. 25:316–329. https://doi.org/10.1016/j.tics.2021.01.008.

Hornak J. 2003. Changes in emotion after circumscribed surgical lesions of the orbitofrontal and cingulate cortices. *Brain*. 126:1691–1712. https://doi.org/10.1093/brain/awg168.

Howard MF, Reggia JA. 2007. A theory of the visual system biology underlying development of spatial frequency lateralization. *Brain Cogn*. 64:111–123. https://doi.org/10.1016/j.bandc.2007.01.004.

Jenkinson M, Beckmann CF, Behrens TEJ, Woolrich MW, Smith SM. 2012. FSL. *NeuroImage*. 62:782–790. https://doi.org/10.1016/j.neuroimage.2011.09.015.

Kauffmann L, Ramanoël S, Peyrin C. 2014. The neural bases of spatial frequency processing during scene perception. *Front Integr Neurosci*. 8:37. https://doi.org/10.3389/fnint.2014.00037.

Kret ME, de Gelder B. 2010. Social context influences recognition of bodily expressions. *Exp Brain Res*. 203:169–180. https://doi.org/10.1007/s00221-010-2220-8.

Kret ME, Pichon S, Grèzes J, de Gelder B. 2011. Similarities and differences in perceiving threat from dynamic faces and bodies. *An fMRI study NeuroImage*. 54:1755–1762. https://doi.org/10.1016/j.neuroimage.2010.08.012.

Kret ME, Roelofs K, Stekelenburg JJ, de Gelder B. 2013. Emotional signals from faces, bodies and scenes influence observers' face expressions, fixations and pupil-size. *Front Hum Neurosci*. 7:810. https://doi.org/10.3389/fnhum.2013.00810.

Kriegeskorte N, Goebel R, Bandettini P. 2006. Information-based functional brain mapping. *Proc Natl Acad Sci*. 103:3863–3868. https://doi.org/10.1073/pnas.0600244103.

Lanzilotto M et al. 2025. Learning to fear novel stimuli by observing others in the social affordance framework. *Neurosci Biobehav Rev*. 169:106006. https://doi.org/10.1016/j.neubiorev.2025.106006.

LeDoux JE. 1998. *The emotional brain: the mysterious underpinnings of emotional life*. New York City, United States: Simon and Schuster.

LeDoux JE. 2000. Emotion circuits in the brain. *Annu Rev Neurosci*. 23:155–184. https://doi.org/10.1146/annurev.neuro.23.1.155.

Liang Y, Liu B, Ji J, Li X. 2019. Network representations of facial and bodily expressions: evidence from multivariate connectivity pattern classification. *Front Neurosci*. 13:1111. https://doi.org/10.3389/fnins.2019.01111.

Livingstone M, Hubel D. 1988. Segregation of form, color, movement, and depth: anatomy, physiology, and perception. *Science*. 240:740–749. https://doi.org/10.1126/science.3283936.

Lyon DC, Kaas JH. 2001. Connectional and architectonic evidence for dorsal and ventral V3, and dorsomedial area in marmoset monkeys. *J Neurosci*. 21:249–261. https://doi.org/10.1523/JNEUROSCI.21-01-00249.2001.

McFadyen J, Mermillod M, Mattingley JB, Halász V, Garrido MI. 2017. A rapid subcortical amygdala route for faces irrespective of spatial frequency and emotion. *J Neurosci*. 37:3864–3874. https://doi.org/10.1523/JNEUROSCI.3525-16.2017.

McFadyen J, Mattingley JB, Garrido MI. 2019. An afferent white matter pathway from the pulvinar to the amygdala facilitates fear recognition. *elife*. 8:e40766. https://doi.org/10.7554/eLife.40766.

Megías-Robles A et al. 2020. The 'reading the mind in the eyes' test and emotional intelligence. Royal Society open. *Science*. 7:201305. https://doi.org/10.1098/rsos.201305.

Meletti S et al. 2012. 2012 fear and happiness in the eyes: an intra-cerebral event-related potential study from the human amygdala. *Neuropsychologia*. 50:44–54. https://doi.org/10.1016/j.neuropsychologia.2011.10.020.

Méndez CA et al. 2022. A deep neural network model of the primate superior colliculus for emotion recognition. *Philos Trans R Soc B Biol Sci*. 377:20210512. https://doi.org/10.1098/rstb.2021.0512.

Méndez-Bértolo C et al. 2016. A fast pathway for fear in human amygdala. *Nat Neurosci*. 19:1041–1049. https://doi.org/10.1038/nn.4324.

Merigan WH, Maunsell JH. 1993. How parallel are the primate visual pathways? *Annu Rev Neurosci*. 16:369–402. https://doi.org/10.1146/annurev.ne.16.030193.002101.

Mermillod M, Bonin P, Mondillon L, Alleysson D, Vermeulen N. 2010. Coarse scales are sufficient for efficient categorization of emotional facial expressions: evidence from neural computation. *Neurocomputing*. 73:2522–2531. https://doi.org/10.1016/j.neucom.2010.06.002.

Milner AD, Goodale MA. 2008. Two visual systems re-viewed. *Neuropsychologia*. 46:774–785. https://doi.org/10.1016/j.neuropsychologia.2007.10.005.

Mobbs D et al. 2007. When fear is near: threat imminence elicits prefrontal-periaqueductal gray shifts in humans. *Science*. 317:1079–1083. https://doi.org/10.1126/science.1144298.

Nassi JJ, Callaway EM. 2009. Parallel processing strategies of the primate visual system. *Nat Rev Neurosci*. 10:360–372. https://doi.org/10.1038/nrn2619.

Niedenthal PM, Mermillod M, Maringer M, Hess U. 2010. The simulation of smiles (SIMS) model: embodied simulation and the meaning of facial expression. *Behav Brain Sci*. 33:417–433. https://doi.org/10.1017/S0140525X10000865.

Noble WS. 2006. What is a support vector machine? *Nat Biotechnol*. 24:1565–1567. https://doi.org/10.1038/nbt1206-1565.

Oliva A, Schyns PG. 1997. Coarse blobs or fine edges? Evidence that information Diagnosticity changes the perception of complex visual stimuli. *Cognit Psychol*. 34:72–107. https://doi.org/10.1006/cogp.1997.0667.

Palagi E, Celeghin A, Tamietto M, Winkielman P, Norscia I. 2020. The neuroethology of spontaneous mimicry and emotional contagion in human and non-human animals. *Neurosci Biobehav Rev*. 111:149–165. https://doi.org/10.1016/j.neubiorev.2020.01.020.

Palomero-Gallagher N, Amunts K. 2022. A short review on emotion processing: a lateralized network of neuronal networks. *Brain Struct Funct*. 227:673–684. https://doi.org/10.1007/s00429-021-02331-7.

Paschali M, Zhao Q, Adeli E, Pohl KM. 2022. Bridging the gap between deep learning and hypothesis-driven analysis via permutation testing. In: Rekik I, Adeli E, Park SH, Cintas C, editors. *Predictive intelligence in medicine*. Vol. 13564. Springer Nature Switzerland (Lecture Notes in Computer Science), Cham. pp 13–23 [Accessed 2024 October 31, 2024]. https://link.springer.com/10.1007/978-3-031-16919-9_2.

Pavlova MA. 2012. Biological motion processing as a Hallmark of social cognition. *Cereb Cortex*. 22:981–995. https://doi.org/10.1093/cercor/bhr156.

Pessoa L, Adolphs R. 2010. Emotion processing and the amygdala: from a "low road" to "many roads" of evaluating biological significance. *Nat Rev Neurosci*. 11:773–782. https://doi.org/10.1038/nrn2920.

Peyrin C, Chauvin A, Chokron S, Marendaz C. 2003. Hemispheric specialization for spatial frequency processing in the analysis of natural scenes. *Brain Cogn*. 53:278–282. https://doi.org/10.1016/S0278-2626(03)00126-X.

Phelps EA, LeDoux JE. 2005. Contributions of the amygdala to emotion processing: from animal models to human behavior. *Neuron*. 48:175–187. https://doi.org/10.1016/j.neuron.2005.09.025.

Phillips ML, Drevets WC, Rauch SL, Lane R. 2003. Neurobiology of emotion perception II: implications for major psychiatric disorders. *Biol Psychiatry*. 54:515–528. https://doi.org/10.1016/S0006-3223(03)00171-9.

Pitcher D, Ungerleider LG. 2021. Evidence for a third visual pathway specialized for social perception. *Trends Cogn Sci*. 25:100–110. https://doi.org/10.1016/j.tics.2020.11.006.

Pourtois G, Dan ES, Grandjean D, Sander D, Vuilleumier P. 2005. Enhanced extrastriate visual response to bandpass spatial frequency filtered fearful faces: time course and topographic evoked-potentials mapping. *Hum Brain Mapp*. 26:65–79. https://doi.org/10.1002/hbm.20130.

Prins N, Kingdom FAA. 2018. Applying the model-comparison approach to test specific research hypotheses in psychophysical research using the Palamedes toolbox. *Front Psychol*. 9:1250. https://doi.org/10.3389/fpsyg.2018.01250.

Proverbio AM, Zani A, Avella C. 1997. Hemispheric asymmetries for spatial frequency discrimination in a selective attention task. *Brain Cogn*. 34:311–320. https://doi.org/10.1006/brcg.1997.0901.

Rizzolatti G, Sinigaglia C. 2016. The mirror mechanism: a basic principle of brain function. *Nat Rev Neurosci*. 17:757–765. https://doi.org/10.1038/nrn.2016.135.

Rotshtein P, Vuilleumier P, Winston J, Driver J, Dolan R. 2007. Distinct and convergent visual processing of high and low spatial frequency information in faces. *Cereb Cortex*. 17:2713–2724. https://doi.org/10.1093/cercor/bhl180.

Ruiz-Soler M, Beltran FS. 2006. Face perception: an integrative review of the role of spatial frequencies. *Psychol Res Psychol Forsch*. 70:273–292. https://doi.org/10.1007/s00426-005-0215-z.

Sander D, Grafman J, Zalla T. 2003. The human amygdala: an evolved system for relevance detection. *Rev Neurosci*. 14:303–316. https://doi.org/10.1515/REVNEURO.2003.14.4.303.

Schiano Lomoriello A et al. 2024. Sensitivity to basic emotional expressions and the emotion perception space in the absence of facial mimicry: the case of individuals with congenital facial palsy. *Emotion*. 24:602–616. https://doi.org/10.1037/emo0001275.

Schiano Lomoriello A, Cantoni C, Ferrari PF, Sessa P. 2023. Close to me but unreachable: spotting the link between peripersonal space and empathy. *Soc Cogn Affect Neurosci*. 18:1–12. https://doi.org/10.1093/scan/nsad030.

Schyns PG, Oliva A. 1999. Dr. angry and Mr. smile: when categorization flexibly modifies the perception of faces in rapid visual presentations. *Cognition*. 69:243–265. https://doi.org/10.1016/S0010-0277(98)00069-9.

Sessa P et al. 2022. Degenerate pathway for processing smile and other emotional expressions in congenital facial palsy: an hdEEG investigation. *Philos Trans R Soc B Biol Sci*. 377:20210190. https://doi.org/10.1098/rstb.2021.0190.

Sinke CB, Sorger B, Goebel R, de Gelder B. 2010. Tease or threat? Judging social interactions from bodily expressions. *NeuroImage*. 49:1717–1727. https://doi.org/10.1016/j.neuroimage.2009.09.065.

Skottun BC. 2015. On the use of spatial frequency to isolate contributions from the magnocellular and parvocellular systems and the dorsal and ventral cortical streams. *Neurosci Biobehav Rev*. 56:266–275. https://doi.org/10.1016/j.neubiorev.2015.07.002.

Soon CS, Namburi P, Chee MW. 2013. Preparatory patterns of neural activity predict visual category search speed. *NeuroImage*. 66:215–222. https://doi.org/10.1016/j.neuroimage.2012.10.036.

Stein T, Seymour K, Hebart MN, Sterzer P. 2014. Rapid fear detection relies on high spatial frequencies. *Psychol Sci*. 25:566–574. https://doi.org/10.1177/0956797613512509.

Tamietto M, de Gelder B. 2008. Emotional contagion for unseen bodily expressions: Evidence from facial EMG. In: *2008 8th IEEE international conference on Automatic Face & Gesture Recognition*. Amsterdam, Netherlands: IEEE. p. 1–5.

Tamietto M, de Gelder B. 2010. Neural bases of the non-conscious perception of emotional signals. *Nat Rev Neurosci*. 11:697–709. https://doi.org/10.1038/nrn2889.

Tamietto M et al. 2009. Unseen facial and bodily expressions trigger fast emotional reactions. *Proc Natl Acad Sci USA*. 106:17661–17666. https://doi.org/10.1073/pnas.0908994106.

Tamietto M, Pullens P, de Gelder B, Weiskrantz L, Goebel R. 2012. Subcortical connections to human amygdala and changes following destruction of the visual cortex. *Curr Biol*. 22:1449–1455. https://doi.org/10.1016/j.cub.2012.06.006.

Tamietto M et al. 2015. Once you feel it, you see it: insula and sensory-motor contribution to visual awareness for fearful bodies in parietal neglect. *Cortex*. 62:56–72. https://doi.org/10.1016/j.cortex.2014.10.009.

Van den Stock J et al. 2011. Cortico-subcortical visual, somatosensory, and motor activations for perceiving dynamic whole-body emotional expressions with and without striate cortex (V1). *Proc Natl Acad Sci*. 108:16188–16193. https://doi.org/10.1073/pnas.1107214108.

Van den Stock J et al. 2014. Neural correlates of body and face perception following bilateral destruction of the primary visual cortices. *Front Behav Neurosci*. 8:30. https://doi.org/10.3389/fnbeh.2014.00030.

Van Overwalle F, Baetens K, Mariën P, Vandekerckhove M. 2014. Social cognition and the cerebellum: a meta-analysis of over 350 fMRI studies. *NeuroImage*. 86:554–572. https://doi.org/10.1016/j.neuroimage.2013.09.033.

Vuilleumier P, Armony JL, Driver J, Dolan RJ. 2003. Distinct spatial frequency sensitivities for processing faces and emotional expressions. *Nat Neurosci*. 6:624–631. https://doi.org/10.1038/nn1057.

Wager TD, Phan KL, Liberzon I, Taylor SF. 2003. Valence, gender, and lateralization of functional brain anatomy in emotion: a meta-analysis of findings from neuroimaging. *NeuroImage*. 19:513–531. https://doi.org/10.1016/S1053-8119(03)00078-8.

Weaverdyck ME, Lieberman MD, Parkinson C. 2020. Tools of the trade multivoxel pattern analysis in fMRI: a practical introduction for social and affective neuroscientists. *Soc Cogn Affect Neurosci*. 15:487–509. https://doi.org/10.1093/scan/nsaa057.

Winston JS, Vuilleumier P, Dolan RJ. 2003. Effects of low-spatial frequency components of fearful faces on fusiform cortex activity. *Curr Biol*. 13:1824–1829. https://doi.org/10.1016/j.cub.2003.09.038.

Xu Y, Chun MM. 2009. Selecting and perceiving multiple visual objects. *Trends Cogn Sci*. 13:167–174. https://doi.org/10.1016/j.tics.2009.01.008.

Ying X. 2019. An overview of overfitting and its solutions. *J Phys Conf Ser*. 1168:022022. https://doi.org/10.1088/1742-6596/1168/2/022022.

Yue X, Tjan BS, Biederman I. 2006. What makes faces special? *Vis Res*. 46:3802–3811. https://doi.org/10.1016/j.visres.2006.06.017.

Zhao D, Shen X, Li S, He W. 2023. The impact of spatial frequency on the perception of crowd emotion: an fMRI study. *Brain Sci*. 13:1699. https://doi.org/10.3390/brainsci13121699.